Microphase Separation in Graft Copolymer Membranes with Pendant Oligodimethylsiloxanes and Their Permselectivity for Aqueous Ethanol Solutions

Takashi Miyata,* Toru Takagi, and Tadashi Uragami*

Chemical Branch, Faculty of Engineering, Kansai University, Suita, Osaka 564, Japan

Received May 6, 1996; Revised Manuscript Received September 13, 1996[⊗]

ABSTRACT: Graft copolymer membranes consisting of both ethanol- and water-permselective components for the separation of aqueous ethanol solutions were prepared by the copolymerization of an oligodimethylsiloxane (DMS) macromonomer with methyl methacrylate (MMA). This paper describes the relationship between microphase separation in MMA-*g*-DMS membranes and their permselectivity for aqueous ethanol solutions by pervaporation. The MMA-*g*-DMS membranes changed drastically from water to ethanol permselective according to the DMS content. Using a transmission electron microscope, appreciable microphase separation was observed in the MMA-*g*-DMS membranes. The change in the permselectivity of the MMA-*g*-DMS membranes could be explained by morphological changes in the microphase separation, based on Maxwell's model and a combined model consisting of both parallel and series models. Furthermore, image processing of the transmission electron micrographs enabled us to reveal the percolation transition of the DMS phase at a DMS content of about 40 mol %. These results suggest that the continuity of DMS phases in the microphase separation of MMA-*g*-DMS membranes directly affects their permselectivity for aqueous ethanol solutions.

Introduction

Membrane techniques with potential savings in energy costs are useful for the separation of organic liquid mixtures which cannot be completely separated by the distillation method because of azeotropy and similar boiling points. Pervaporation, in which the permeate undergoes a phase change from liquid to vapor through a membrane, is one of these membrane techniques.[1] Pervaporation membranes for the separation of aqueous ethanol solutions have been developed rigorously, since the separation of ethanol and water is very important for the commercial production of alcohol. There are two types of pervaporation membranes, water- and ethanol-permselective membranes, which preferentially permeate water and ethanol from aqueous ethanol solutions, respectively. In pervaporation the permeability and permselectivity of a membrane are dependent on both the solubility and diffusivity of the permeants in the membrane.

Poly(dimethylsiloxane) (PDMS) and poly[1-(trimethylsilyl)-1-propyne] (PTMSP) membranes are representative ethanol-permselective membranes used in the separation of aqueous ethanol solutions by pervaporation. The ethanol permselectivities of these membranes are attributable to a stronger affinity for ethanol than for water and to relatively high diffusivity of ethanol through the membranes. However, these membranes have a few disadvantages such as weak mechanical strength or low stability which must be overcome for industrial utility in the separation of aqueous ethanol solutions. In order to ameliorate these disadvantages, many workers have introduced a component with strong mechanical properties into the PDMS and PTMSP membranes.[2−7] Enhancement of the ethanol permselectivity of their membranes has also been desirable for the development of a highly efficient ethanol-permselective membrane. Introducing hydrophobic components, especially fluorine-containing components, into PDMS and PTMSP membranes by copolymerization or blending is one method for improving the ethanol permselectivity through lowering affinity for water. For example, Nagase et al. prepared excellent ethanol-permselective membranes by chemically introducing trialkylsilyl groups, fluoroalkyl groups, and so on into the PTMSP membrane.[4−7]

Multicomponent polymer membranes, such as copolymer membranes or polymer blend membranes, have attracted much attention, since a variety of functional components can be combined into single membrane.[8−11] In most multicomponent polymer membranes, however, micro- or macrophase separation often takes place due to the very small entropy and positive heat of mixing. Since such phase separation directly affects membrane properties, closely relating phase separation in the membranes to their permeability and permselectivity is important for the development of multicomponent polymer membranes with high-performance.

Some studies of gas permeation through multicomponent polymer membranes have considered the phase-separated morphology of the membranes.[12−24] Robeson et al.[16,17] prepared two types of copolymer membranes, random and block copolymer membranes, consisting of styrene and methacrylonitrile, and investigated oxygen permeation through these membranes. There was a distinct difference in oxygen permeability between the block and random copolymer membranes. This difference was due to the fact that phase separation in the block copolymer membranes affected the oxygen permeability. Gas permeation through siloxane−imide block copolymer membranes having microphase separation has been evaluated by considering the arrangements of glassy and rubbery phases as well as membrane composition.[18] The relationship between microphase separation in the membranes and gas permeation has also been studied on the basis of a variety of models.[12−15] These models have indicated that gas permeability is closely dependent on membrane morphology.

* To whom correspondence should be addressed.

[⊗] Abstract published in *Advance ACS Abstracts,* November 1, 1996.

S0024-9297(96)00663-8 CCC: $12.00

On the other hand, in the separation of organic liquid mixtures by pervaporation, only a few studies have described the effect of microphase separation on membrane permselectivity. Kerres et al.[25] studied permeability and permselectivity for aqueous ethanol solutions through AB-cross-linked copolymer membranes consisting of elastomeric and glassy components in terms of membrane microphase separation. Studies of water vapor permeation through these membranes by pervaporation revealed that a percolation transition took place in the microphase separation of the membranes. Morphological changes in the membranes caused a drastic change in the permselectivity at the percolation point. Thus, microphase separation in pervaporation membranes has a more marked influence on permeability and permselectivity than that in gas permeation membranes. Consequently, closely relating microphase separation in pervaporation membranes to permselectivity for aqueous ethanol solutions, by the application of various structural models, is important.

Previously, we introduced a variety of components into the PDMS membrane to combine the ethanol permselectivity of the PDMS membrane and the mechanical strength of other components into a single membrane. PDMS/polystyrene (PSt) interpenetrating polymer network (IPN) membranes were prepared by the bulk copolymerization of styrene (St) and divinylbenzene in PDMS networks in a mold.[26] The mechanical strength of the PDMS membrane could be improved by the introduction of the PSt component. The PDMS/PSt membranes showed ethanol permselectivity regardless of DMS content, when aqueous ethanol solutions permeated the membranes. Permeation and separation through the PDMS/PSt membranes were discussed from the viewpoint of microphase separation in the membranes. The graft copolymer membranes prepared by the copolymerization of methyl methacrylate (MMA) and DMS macromonomer showed water permselectivity when DMS content was low and ethanol permselectivity when DMS content was high.[27] These observations suggested that the microphase separation in the graft copolymer membranes may affect their permselectivity. Therefore, it is important to investigate the morphology of microphase separation in graft copolymer membranes in more detail.

Our aim in this study is to closely relate the morphology of microphase separation in two-component polymer membranes to their permeability and permselectivity for aqueous ethanol solutions. Two membrane materials having different permselectivities were selected. MMA and DMS which are water and ethanol permselective, respectively, were used to synthesize graft copolymers (MMA-*g*-DMS) by copolymerizing MMA with DMS macromonomer. Permeation and separation of aqueous ethanol solutions through the MMA-*g*-DMS membranes were then investigated by pervaporation. The relationship between the morphology of the microphase separation in the MMA-*g*-DMS membranes and membrane properties was revealed by investigating morphological changes in the microphase separation on the basis of copolymer composition. Two types of structural models were applied for evaluating permeability, and transmission electron micrograph image processing was used to investigate these changes in detail.

Experimental Section

Materials. Oligodimethylsiloxane (DMS) macromonomer, which has 81 units of pendant DMS as shown below, was supplied by Toray Dow Corning Silicone Co., Ltd. Methyl

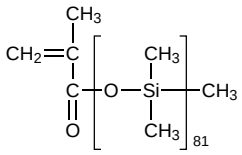

DMS macromonomer

metacrylate (MMA) as a comonomer was purified by distillation under reduced pressure in nitrogen gas. 2,2′-Azobis(isobutyronitrile) (AIBN) recrystallized from benzene solution was used as an initiator. The other solvents and reagents were of analytical grade obtained from commercial sources and were used without further purification.

Copolymerization of DMS Macromonomer with MMA. DMS macromonomer and MMA in a typical composition were dissolved together with AIBN (0.5 wt % relative to the monomers) in benzene to make a 40 wt % solution. The mixture was then transferred to a glass tube. The copolymerization was carried out at 60 °C for 6 h under nitrogen gas. The resulting MMA-*g*-DMS was isolated by slow precipitation with a 1:2 mixture of *n*-hexane and ethanol. It was purified by reprecipitation from benzene solution into a 1:2 mixture of *n*-hexane and ethanol, and dried at 40 °C *in vacuo*.

Average molecular weights of MMA-*g*-DMS were determined by gel permeation chromatography (GPC) (Waters Associate Inc.; R-400), equipped with a TSK-GEL column (Tosoh Co. Ltd.; G2000HXL, G3000HXL, G5000HXL) and ultraviolet spectrophotometry (Shimadzu Co. Ltd.; SPD-2A). Tetrahydrofuran was used as an eluent and the calibration was made with polystyrene standards. Number-average molecular weights of MMA-*g*-DMS range between about 60 000 and 75 000 g/mol. The ratio of the weight-average molecular weight to the number-average molecular weight (M_w/M_n) was greater than 2. This indicates that the molecular weight of MMA-*g*-DMS is polydispersive.

The composition of the resulting MMA-*g*-DMS was determined from 400 MHz ^{1}H nuclear magnetic resonance (NMR) (JEOL; GSX-400) spectra by measuring the integrals of the peaks assigned to methyl protons (3.5 ppm) of the MMA and DMS protons (0 ppm) of the DMS macromonomer, after the purified copolymer had been dissolved in chloroform-*d* containing 1 vol % tetramethylsilane (TMS). The DMS content in MMA-*g*-DMS was slightly lower than that in the feed. Since the molecular size of the DMS macromonomer is much greater than that of MMA, the former is more difficult to polymerize than the latter due to steric hindrance of long pendant groups. Characterizations of the MMA-*g*-DMS copolymer are summarized in Table 1.

Membrane Preparation. Prescribed amounts of MMA-*g*-DMS were dissolved in benzene at 25 °C at a concentration of 4 wt % for the preparation of casting solutions. The MMA-*g*-DMS membranes were prepared by pouring the casting solutions onto rimmed glass plates and allowing the solvent to evaporate completely at 25 °C. The resulting membranes were transparent and their thickness was about 40 μm.

Transmission Electron Micrographs (TEM). The MMA-*g*-DMS membranes were vapor-stained with an aqueous solution of 5 wt % RuO_4 in glass-covered dishes.[28] The stained membranes were embedded in epoxy resin and cross sectioned into thin films (thickness approximately 60 nm) with a microtome (Leica; Reichert Ultracut E). The morphological features that can be brought out by our staining procedure were observed with a transmission electron microscope (TEM) (JEOL JEM-1210) at an accelerating voltage of 80 kV.

Permeation Measurements. Pervaporation was carried out using the apparatus as shown in Figure 1[19−32] under the following conditions: permeation temperature, 40 °C; pressure of permeate side, 1×10^{-2} Torr. The effective membrane area was 13.8 cm^2. An aqueous solution of 10 wt % ethanol was used as a feed solution. The compositions of the feed solution and permeate were determined using a gas chromatography (Shimadzu GC-9A) equipped with a flame ionization detector (FID) and capillary column (Shimadzu Co. Ltd.; Shimalite F)

Table 1. Result of the Copolymerization of MMA with DMS Macromonomer[a]

macromonomer feed		molecular weight[b]			graft copolymer[c]		
DMS units (mol %)	macromonomer (mol %)	$\overline{M_n}$	$\overline{M_w}$	$\overline{M_w}/\overline{M_n}$	DMS units (mol %)	macromonomer (mol %)	volume fraction of DMS
40	0.82	6.58×10^4	1.74×10^5	2.64	30	0.54	0.29
50	1.22	6.59×10^4	1.72×10^5	2.62	34	0.65	0.33
60	1.82	6.01×10^4	1.14×10^5	1.90	52	1.30	0.49
70	2.80	7.44×10^4	1.52×10^5	2.04	68	2.51	0.66

[a] [Total monomer] = 40 wt %, [AIBN] = 5×10^{-3} wt % at 60 °C in benzene. [b] Determined by GPC calibrated with polystyrene standard. [c] Determined by ^{1}H NMR.

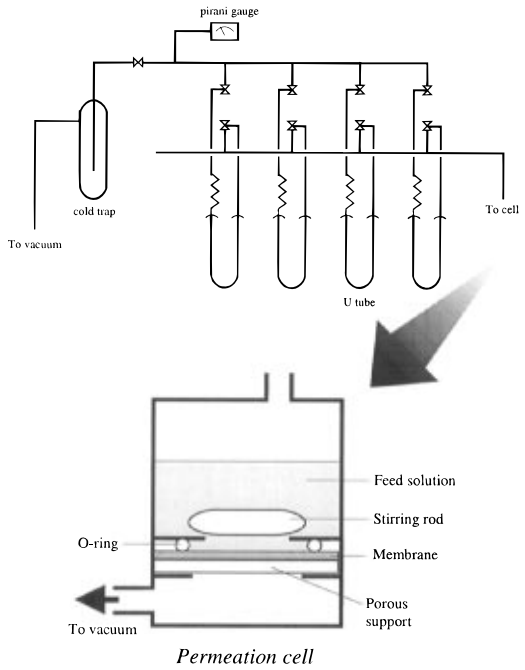

Figure 1. Pervaporation apparatus.

heated to 200 °C. The separation factor, α_{EtOH/H_2O}, was calculated from the ethanol concentration in the feed solution and permeate using eq 1, where P_{EtOH} and P_{H_2O} are the ethanol

$$\alpha_{EtOH/H_2O} = \frac{P_{EtOH}/P_{H_2O}}{F_{EtOH}/F_{H_2O}} \quad (1)$$

and water composition in the permeate, and F_{EtOH} and F_{H_2O} are those in the feed solution, respectively. The permeation rates of an aqueous ethanol solution in pervaporation were determined from the weight of the permeate collected in a cold trap, permeation time, and effective membrane area.

The results of the permeation of an aqueous ethanol solution by pervaporation were reproducible and the errors inherent in the permeation measurements are of the order of a few percent.

Results and Discussion

Pervaporation Characteristics of MMA-g-DMS membranes. Figure 2 shows the effect of DMS content on the separation factor and the normalized permeation rate through the MMA-*g*-DMS membranes by pervaporation. In this figure, the normalized permeation rate is the product of the permeation rate and the membrane thickness. Increasing DMS content tended to increase the normalized permeation rate. Glass transition temperatures of DMS and MMA homopolymers are about −127 and 128 °C, respectively.[27] Therefore, the diffusivity of the permeants in the rubbery DMS component is much higher than that in the glassy MMA component. The higher diffusivity of the permeants in the DMS component causes an increase in the normalized permeation rate with increased DMS content. Furthermore, the normalized permeation rate exhibited a drastic increase at a DMS content of about 40 mol %. This implies that the structures of MMA-*g*-DMS membranes change remarkably at this DMS content.

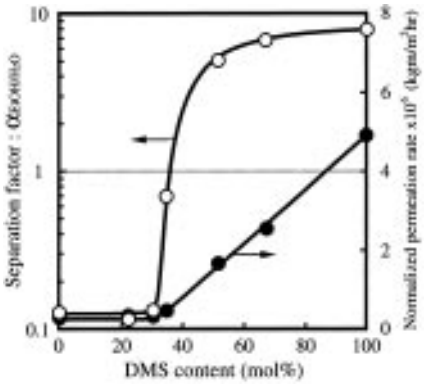

Figure 2. Effect of the DMS content on the separation factor (○) and the normalized permeation rate (●) through the MMA-*g*-DMS membranes by pervaporation. Feed solution: aqueous solution of 10 wt % ethanol (40 °C). Dashed line represents the feed composition.

As can be seen from Figure 2, the separation factor through the MMA-*g*-DMS membranes with a DMS content of less than 40 mol % was less than 1. This indicates that the water from an aqueous ethanol solution preferentially permeates the membrane by pervaporation. With increasing DMS content, however, the separation factor gradually increases until it becomes approximately 7. The fact that the separation factor is more than 1 indicates that the MMA-*g*-DMS membranes become ethanol permselective with the increase in DMS content. These results are attributable to an increase in both the hydrophobicity of the membrane and the diffusivity of the ethanol molecule as DMS content increases; since the DMS component is hydrophobic, it has a stronger affinity for ethanol molecules than for water molecules. Therefore, the DMS component preferentially incorporates more ethanol molecules than water molecules. Furthermore, the diffusivity of the ethanol molecule in the rubbery DMS component may be similar to that of the water molecule due to considerably free rotation of the siloxane bone. As a result of both the higher solubility of ethanol and the diffusivity of ethanol comparable to water in the DMS component, the ethanol permselectivity of the MMA-*g*-DMS membranes is enhanced with increased DMS content. Such changes in the permselectivity with copolymer composition are not common in the separation of aqueous alcohol solutions through polymer membranes by pervaporation. The DMS content with which the MMA-*g*-DMS membrane changes from water to ethanol permselective corresponds to the content with which the normalized permeation rate increases sharply. These results have led us to speculate that the mem-

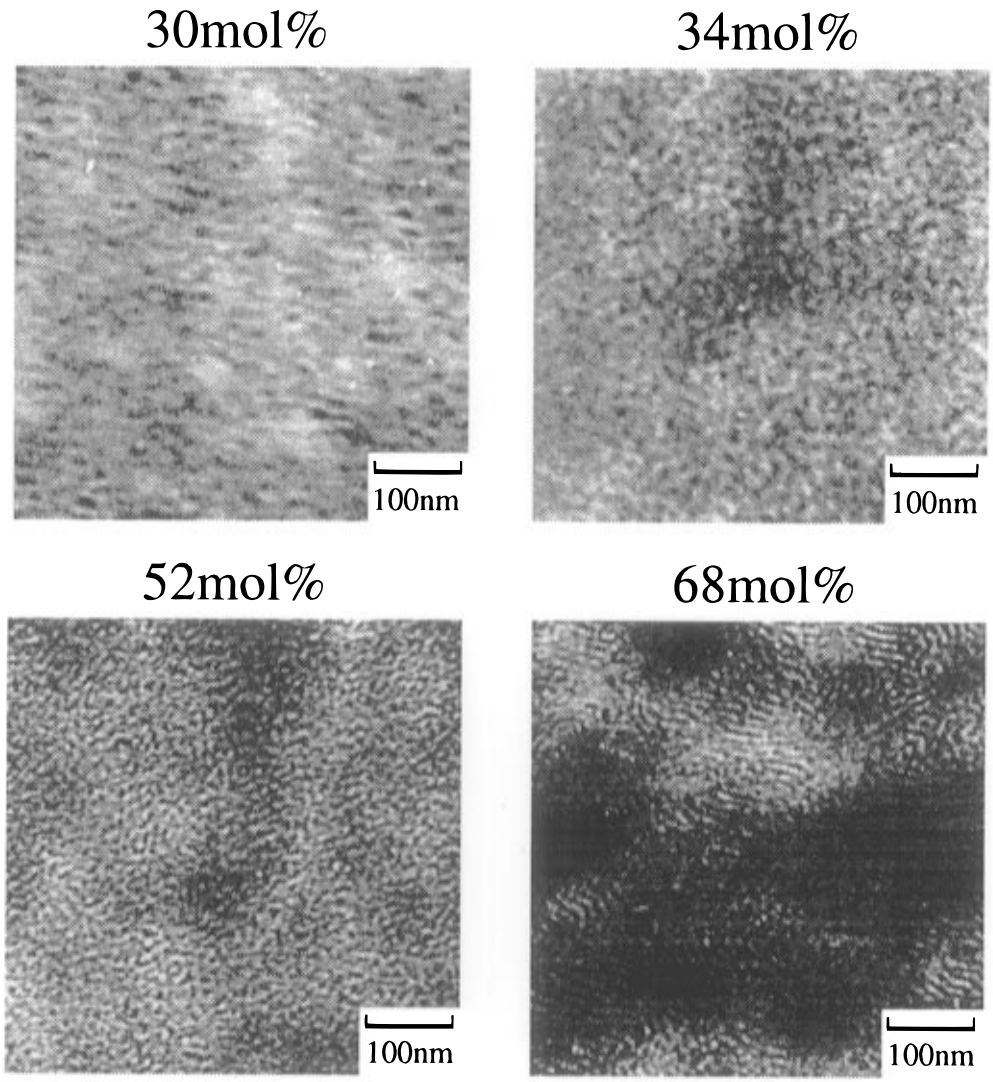

Figure 3. Transmission electron micrographs of cross sections of MMA-*g*-DMS membranes with various DMS contents. The dark region stained by RuO_4 represents a DMS component.

brane structures changes remarkably at a DMS content of about 40 mol %.

Microphase Separation in MMA-g-DMS Membranes. Transmission electron micrographs of cross sections of the MMA-*g*-DMS membranes with various DMS contents are shown in Figure 3. The DMS component was stained by RuO_4 but the MMA component was not. These micrographs demonstrated that the MMA-*g*-DMS membranes have distinct phases of microphase separation consisting of a DMS phase and a MMA phase, regardless of the DMS content. The dark region stained by RuO_4, the DMS phase, increased with the DMS content. Furthermore, the microphase separation of the MMA-*g*-DMS membranes appears to change by the DMS content. Such a change in the morphology of microphase separation in the MMA-*g*-DMS membranes may cause the drastic changes in the permeability and permselectivity for aqueous ethanol solutions. Therefore, the results of pervaporation for an aqueous ethanol solution must be evaluated in more detail from the perspective of morphological changes in the MMA-*g*-DMS membranes.

Two Types of Structural Models for Permeability. In general, gas permeation behavior through a membrane consisting of glassy and rubbery components is strongly dependent on the arrangement of glassy and rubbery phases. Tsujita et al.[18] discussed the relationship between DMS content and the permeability of CO_2 through microphase-separated siloxane–imide block copolymer membranes on the basis of two types of two-phase models, that is, a parallel model and a series model. In the former, two phases are arranged parallel to the direction of CO_2 permeation. The latter has a structure in which the two phases are arranged perpendicular to the direction of permeation. The total permeability in the parallel model, consisting of phase A and phase B, is represented by eq 2, where ϕ_i and P_i

$$P = \phi_A P_A + \phi_B P_B \tag{2}$$

are the volume fraction and normalized permeation rate for phase *i*, respectively. In the series model, the total permeability is related to the permeability and volume fraction for each phase by eq 3.

$$\frac{1}{P} = \frac{\phi_A}{P_A} + \frac{\phi_B}{P_B} \tag{3}$$

On the basis of this model, we propose a combined model consisting of a parallel model and a series model as shown in Figure 4. In our combined model, the MMA phase is divided into a MMA1 phase and a MMA2 phase in a series. The DMS phase is arranged in series with the MMA1 phase and parallel to the MMA2 phase.

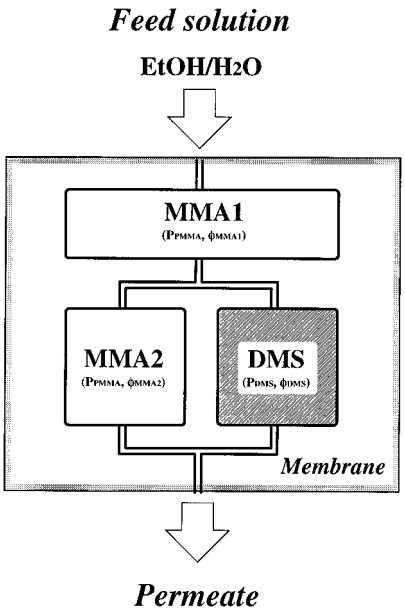

Figure 4. Schematic representation of a combined model consisting of both a series model and a parallel model.

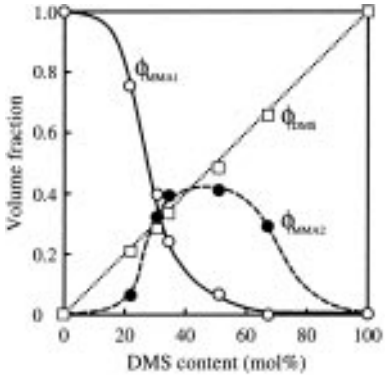

Figure 5. Relationship between the DMS content and the volume fraction of the elements in the combined model composed of both a series model and a parallel model as shown in Figure 4: (○) volume fraction of MMA element in the series model (ϕ_{MMA1}); (●) volume fraction of MMA element in the parallel model (ϕ_{MMA2}); (□) volume fraction of DMS element in the parallel model (ϕ_{DMS}).

Then, the total normalized permeation rate, P, in the combined model is given by eq 4. Contrary to the

$$\frac{1}{P} = \frac{\phi_{MMA1}}{P_{PMMA}} + \frac{\phi_{MMA2} + \phi_{DMS}}{\phi_{MM2}P_{PMMA} + \phi_{DMS}P_{DMS}}$$

$$\phi_{MMA1} + \phi_{MMA2} + \phi_{DMS} = 1 \qquad (4)$$

calculation of permeability by Tsujita et al.,[18] we determined the volume fraction of each phase from the experimental normalized permeation rates (P, P_{PMMA}, P_{PDMS}) of an aqueous ethanol solution using eq 4. The results are shown in Figure 5. Predictably, the calculated volume fraction of the DMS phase increases with DMS content. More remarkable is the volume fraction of the MMA1 phase which is arranged in series with the DMS phase. The volume fraction of the MMA1 phase exhibits a sharp decrease with increasing DMS content and approaches zero at a DMS content above 40 mol %. This means that the structural model for the MMA-*g*-DMS membranes changes from a series model to a parallel model with an increase in the DMS content. From the discussion of microphase separation by the combined model, we can easily guess that the DMS phase changes from a discontinuous phase to a continuous phase in the direction of the membrane thickness.

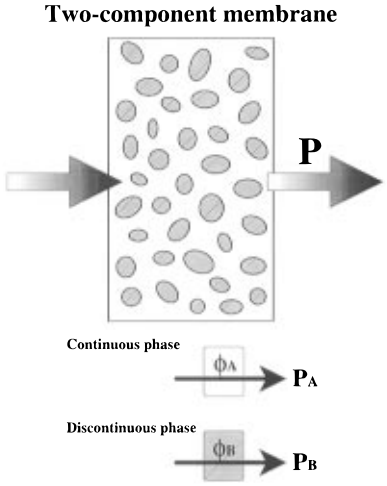

Figure 6. Schematic representation of Maxwell's model for the permeation of aqueous ethanol solutions through membranes with microphase separation consisting of a continuous phase and a discontinuous phase.

In the second structural model, Maxwell's model[12,17] was used to evaluate the permeation of an aqueous ethanol solution through the MMA-*g*-DMS membranes. In general, Maxwell's model[12,17] can be applied to gas permeation through two-component polymer membranes with the microphase separation consisting of a continuous phase and a discontinuous phase as shown in Figure 6. In this study, Maxwell's eq 5 for gas permeation was extended to include the permeation of aqueous ethanol solutions in order to reveal the relationship between microphase separation and permeability

$$P = P_B \frac{P_A + 2P_B - 2\phi_A(P_B - P_A)}{P_A + 2P_B + \phi_A(P_B - P_A)} \qquad (5)$$

where P_A and P_B are the normalized permeation rates of an aqueous ethanol solution in a continuous phase A and a discontinuous phase B, respectively, and ϕ_A is the volume fraction of the continuous phase A.

We assumed two types of morphologies for the microphase separation in MMA-*g*-DMS membranes. The MMA-*g*-DMS membrane was assumed to have microphase separation consisting of a continuous MMA phase and a discontinuous DMS phase or a discontinuous MMA phase and a continuous DMS phase. Theoretical normalized permeation rates of an aqueous ethanol solution were calculated on the basis of this assumption using eq 5. The theoretical normalized permeation rates for Maxwell's model and the experimental values are shown in Figure 7. In the MMA-*g*-DMS membranes with a DMS content of less than 40 mol %, the experimental normalized permeation rates were in fair agreement with the theoretical curves calculated when the MMA phase was assumed to be continuous. Over 40 mol %, however, the experimental normalized permeation rates become higher than the theoretical curves when a continuous MMA phase was assumed and approached the theoretical curves calculated when a continuous DMS phase was assumed. These results suggest that the microphase separation in the MMA-*g*-DMS membrane changes in morphology from a continuous MMA phase and a discontinuous DMS phase

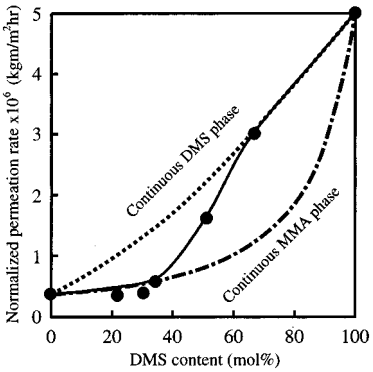

Figure 7. Relationship between the DMS content and normalized permeation rate of an aqueous solution of 10 wt % ethanol through the MMA-*g*-DMS membranes by pervaporation: (- - -) theoretical normalized permeation rate calculated on the assumption that the DMS phase is continuous; (— - —) theoretical normalized permeation rate calculated on the assumption that the MMA phase is continuous, using Maxwell's equation. The closed circles represent experimental normalized permeation rates.

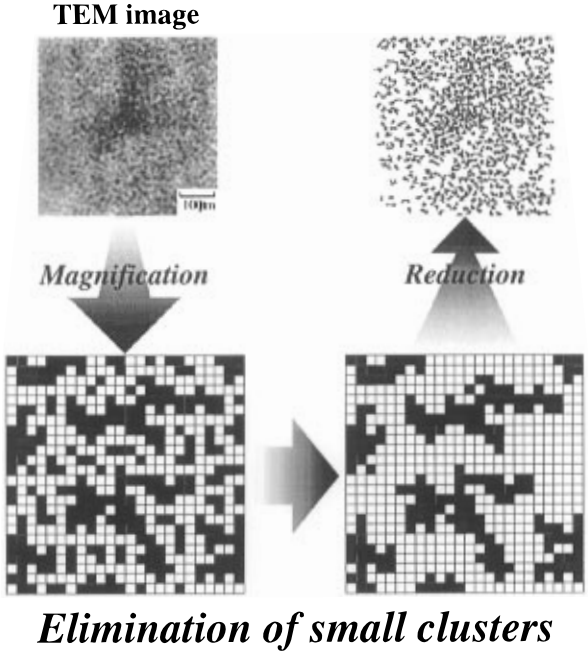

Figure 8. Method for image processing of a transmission electron micrograph.

to that of a continuous DMS phase and discontinuous MMA phase. This suggestion is consistent with the aforementioned conclusion from the combined model consisting of both a parallel and series model. The diffusivity of permeants in the DMS phase is much higher than that in the MMA phase due to the lower glass transition temperature of the DMS component. Therefore, the drastic increase in the permeability of the membranes with a DMS content of more than 40 mol % is attributable to the fact that the DMS component having a high permeability changes from the discontinuous to the continuous phase.

Image Processing of TEM Micrographs. Image processing for TEM micrographs of the MMA-*g*-DMS membranes was performed for a more detailed investigation of the morphology of membrane microphase separation, as shown in Figure 8. The TEM images were transferred to a personal computer and the contrast of the phase separation images was enhanced. Furthermore, the phase separation images were magnified to such an extent that each DMS domain (dark region) could be discriminated. A variety of DMS clusters could be seen in the magnified image. Small DMS clusters made up of less than 12 pixels in the image were eliminated by image processing with the personal computer, and the other larger DMS clusters were left.

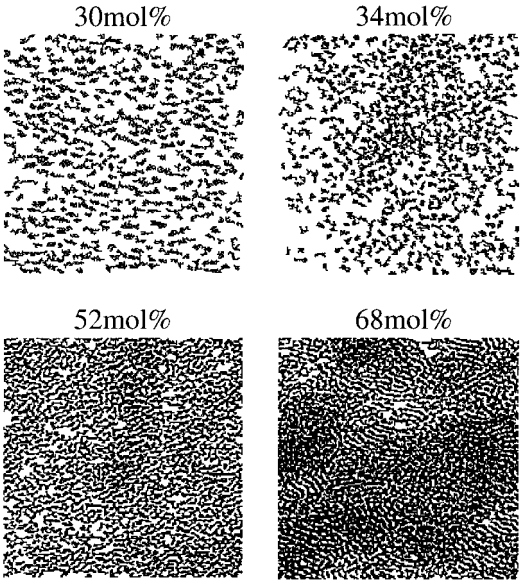

Figure 9. Image processing of transmission electron micrographs of the MMA-*g*-DMS membranes.

The results of the image processing for microphase separation in the MMA-*g*-DMS membranes are shown in Figure 9. By processing these TEM images, it was readily apparent that the DMS clusters grew gradually as DMS content increased. In the MMA-*g*-DMS membranes with a DMS content of less than 40 mol %, a number of DMS clusters of finite sizes (DMS clusters made up of a few pixels) existed. However, when the DMS content increased over 40 mol %, enormous DMS clusters appeared, which were so large that their size could not be defined. These enormous DMS clusters formed a continuous phase in the direction of the membrane thickness. The image processing suggested that the percolation transition of the DMS phase takes place at a DMS content between 30 and 50 mol % (about 40 mol %). This observation supports the morphological changes in the microphase separation predicted from the permeability of an aqueous ethanol solution through the membranes on the basis of both of the structural models. Furthermore, Kerres et al.[25] reported that a copolymer microphase inversion takes place with a percolation point in the region of a PDMS volume fraction of 0.36. Results obtained from the image processing of TEM micrographs were consistent with the percolation point reported by Kerres et al.

Collectively, these observations clearly indicate that the DMS phase changes from a discontinuous phase to a continuous phase by percolation transition at a DMS content of about 40 mol %. Such a percolation transition causes a drastic increase in the permeation rate of an aqueous ethanol solution at a DMS content of 40 mol %. Moreover, these morphological changes can be directly related to permselectivity for an aqueous ethanol solution through the MMA-*g*-DMS membranes by pervaporation.

Relationship between Microphase Separation and Permselectivity. A few studies have investigated the relationship between microphase separation and gas

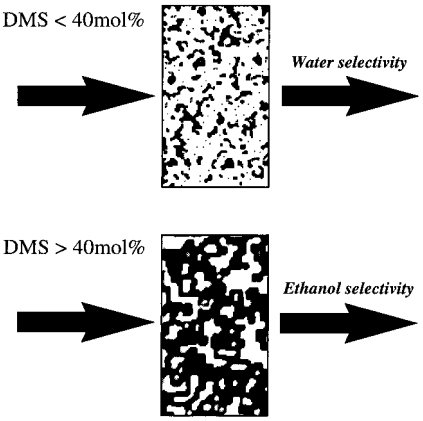

Figure 10. Tentative illustration of the relationship between the microphase separation in MMA-*g*-DMS membranes and their permselectivity for an aqueous ethanol solution.

permeations through polymer membranes.[15−24] However, very few reports have related permselectivity to the morphology of the microphase separation. Our aim is to reveal the relationship between MMA-*g*-DMS membrane morphology and the permselectivity of these membranes for aqueous ethanol solutions, by examining membrane microphase separation from various points of view. This study of membrane morphology has led us to conclude that the microphase inversion takes place at the percolation point with a DMS content of about 40 mol %, at which point the DMS component changes from the discontinuous to the continuous phase.

On the basis of the schematic model, as shown in Figure 10, the changes in the permselectivity of the MMA-*g*-DMS membranes can be explained as follows. As a MMA homopolymer has a high T_g and is a rigid polymer, the diffusivity of molecules in the MMA homopolymer is very low. The diffusivity of ethanol molecules in the membrane is much lower than that of water molecules, because the molecular size of the former is larger than that of the latter. Consequently, the MMA homopolymer membrane shows water permselectivity in the separation of aqueous ethanol solutions by pervaporation despite a stronger affinity for ethanol than for water. Conversely, a DMS homopolymer has a very low T_g and is a rubbery polymer because of the rather free rotation of the siloxane bonds and has high permeability for gases and vapors.[33] Therefore, the diffusivity of the ethanol molecules in the DMS homopolymer may be similar to that of the water molecules. Furthermore, the DMS homopolymer has a relatively stronger affinity for the ethanol molecule than for the water molecule due to its hydrophobicity. Thus, the DMS homopolymer membrane is ethanol permselective in the permeation of aqueous ethanol solutions owing to both high diffusivity and strong affinity.

Consequently, microphase separation in the MMA-*g*-DMS membrane consists of an ethanol-permselective DMS phase and a water-permselective MMA phase. In the membranes with a DMS content of less than 40 mol %, the DMS component is discontinuous in the direction of the membrane thickness. Therefore, as the permeants are mainly diffusing in the continuous MMA phase, the MMA-*g*-DMS membrane becomes water permselective. The DMS phase, however, gradually becomes continuous with increasing DMS content, as revealed previously. The permeants are preferentially diffusing in the DMS phase due to the low T_g of this phase, and the ethanol permselectivity of the DMS phase subsequently becomes more predominant than the water permselectivity of the MMA phase. When DMS content exceeds 40 mol %, the MMA-*g*-DMS membranes become ethanol permselective. Thus, Figure 10 demonstrates that the permeability and permselectivity of the MMA-*g*-DMS membranes are directly correlated with their microphase separation. These results suggest the importance of designing and controlling the morphology of microphase separation in multicomponent polymers in the development of high-performance polymer membranes.

Conclusions

The graft copolymer membranes prepared by the copolymerizations of a DMS macromonomer and MMA had a distinctive microphase separation consisting of a rubbery DMS phase and a glassy MMA phase. In the separation of an aqueous ethanol solution by pervaporation, the permeability and permselectivity of the MMA-*g*-DMS membranes were strongly dependent on the DMS content. In particular, above a DMS content of 40 mol %, the permeability of an aqueous ethanol solution increased drastically and the membranes underwent a change from water to ethanol permselectivity. The pervaporation results could be explained on the basis of morphological changes in the microphase separation of the MMA-*g*-DMS membranes. The application of Maxwell's model and a combined model consisting of both parallel and series models revealed that the DMS component changed from a discontinuous to a continuous phase with increased DMS content. Image processing of TEM micrographs of the MMA-*g*-DMS membranes supported these observations and suggested that the percolation transition of the DMS component takes place at a DMS content of about 40 mol %. Such morphological changes in microphase separation of the MMA-*g*-DMS membranes cause a drastic increase in membrane permeability and a change in permselectivity for aqueous ethanol solutions. These conclusions indicate that the morphology of microphase separation in two-component polymer membranes must be designed and controlled in the development of high-performance pervaporation membranes.

References and Notes

(1) Huang, R. Y. M. *Pervaporation Membrane Separation Processes*; Elsevier: Amsterdam, 1991.
(2) Takegami, S.; Yamada, H.; Tsujii, S. *J. Membr. Sci.* **1922**, *75*, 93.
(3) Okamoto, S.; Butsuen, A.; Tsuru, S.; Nishioka, S.; Tanaka, K.; Kita, H.; Asaoka, S. *Polym. J.* **1987**, *19*, 747.
(4) Ishihara, K.; Nagase, Y.; Matsui, K. *Makromol. Chem., Rapid Commun.* **1986**, *7*, 43.
(5) Nagase, Y.; Mori, S.; Matsui, K. *J. Appl. Polym. Sci.* **1989**, *37*, 1259.
(6) Nagase, Y.; Ishihara, K.; Matsui, K. *J. Polym. Sci., Polym. Phys. Ed.* **1990**, *28*, 377.
(7) Nagase, Y.; Sugimoto, K.; Takamura, Y.; Matsui, K. *J. Appl. Polym. Sci.* **1991**, *43*, 1227.
(8) Kempner, D.; Frisch, K. C. *Polymer Alloys III*; Plenum: New York, 1981.
(9) Aggarwal, S. L. In *Processing, Structure and Properties of Block Copolymers*; Folkes, M. J., Ed.; Elsevier, New York, 1985; p 1.
(10) Paul, D. R. In *Multicomponent Polymer Materials*; Paul, D. R., Sperling, L. H., Eds.; American Chemical Society: Washington, DC, 1986; p 3.
(11) Prentice, P.; Papapostolou, E.; Williams, J. G. In *Multicomponent Polymer Material*; Paul, D. R., Sperling, L. H., Eds.; American Chemical Society: Washington, DC, 1986; p 325.
(12) Crank, J.; Park, G. S. *Diffusion in Polymers*; Academic Press: New York, 1968.
(13) Barrie, J. A.; Munday, K. *J. Membr. Sci.* **1983**, *13*, 175.

(14) Barrie, J. A.; William, M. J. L.; Spencer, H. *J. Membr. Sci.* **1984**, *21*, 185.
(15) Barrie, J. A.; Sagoo, P.; Thomas, A. G. *J. Membr. Sci.* **1989**, *43*, 229.
(16) Robeson, L. M.; Noshay, A.; Matzner, M.; Merriam, C. M. *Angew. Makromol. Chem.* **1973**, *29/30*, 47.
(17) Barnabeo, A. E.; Creasy, W. S.; Robeson, L. M. *J. Polym. Sci., Polym. Chem. Ed.* **1975**, *13*, 1979.
(18) Tsujita, Y.; Yoshimura, K.; Yoshimizu, H.; Takizawa, A.; Kinoshita, T. *Polymer* **1993**, *34*, 2597.
(19) Fujimoto, T.; Ohkoshi, K.; Miyaki, Y.; Nagasawa, M. *J. Membr. Sci.* **1984**, *20*, 313.
(20) Lerma, M. S.; Iwamoto, K.; Seno, M. *J. Appl. Polym., Sci.* **1987**, *33*, 625.
(21) Chiou, J. S.; Paul, D. R. *J. Appl. Polym. Sci.* **1987**, *33*, 2935.
(22) Lee, Y. K.; Tak, T.-M.; Lee, D. S.; Kim, S. C. *J. Membr. Sci.* **1990**, *52*, 157.
(23) Lee, D. S.; Jung, D. S.; Kim, T. H.; Kim, S. C. *J. Membr. Sci.* **1991**, *60*, 233.
(24) Lee, D. S.; Kang, W. K.; An, J. H.; Kim, S. C. *J. Membr. Sci.* **1992**, *75*, 15.
(25) Kerres, J. A.; Strathmann, H. *J. Appl. Polym. Sci.* **1993**, *50*, 1405.
(26) Miyata, T.; Higuchi, J.; Okuno, H.; Uragami, T. *J. Appl. Polym. Sci.* **1996**, *61*, 1315.
(27) Miyata, T.; Takagi, T.; Kadota, T.; Uragami, T. *Macromol. Chem. Phys.* **1995**, *196*, 1211.
(28) Trent, J. S.; Scheinbeim, J. I.; Couchman, P. R. *Macromolecules* **1983**, *16*, 589.
(29) Uragami, T.; Morikawa, T. *Makromol. Chem.* **1989**, *190*, 399.
(30) Uragami, T.; Morikawa, T.; Okuno, H. *Polymer* **1989**, *30*, 1117.
(31) Okuno, H.; Nishimoto, H.; Miyata, T.; Uragami, T. *Makromol. Chem.* **1993**, *194*, 927.
(32) Uragami, T.; Saito, M.; Takigawa, K. *Makromol. Chem., Rapid Commun.* **1988**, *9*, 361.
(33) Noll, W. In *Chemistry and Technology of Silicones*; Academic Press: New York, 1968.

MA960663U